F. Cruz-Peragón, P.J. Casanova-Peláez, R. López-García, J.M. Palomar-Carnicero, **Extending capabilities of Thermal Response Tests in vertical ground heat exchangers: an experiment-based local short-time Temperature Response Factor,** *Applied Thermal Engineering*, 2020, 178, nr. 115606, pp. 1-11, ISSN 1359-4311 (Pergamon-Elsevier, UK), DOI: 10.1016/j.applthermaleng.2020.115606;

Extending capabilities of Thermal Response Tests in vertical ground heat exchangers: an experiment-based local short-time temperature response factor [abbreviated title: an experiment-based STGF from TRT]

Fernando Cruz-Peragón*[1], Pedro J. Casanova-Peláez[2], Rafael López-García[1], José M. Palomar-Carnicero[1]

[1]*Department of Mechanical and Mining Engineering, EPS de Jaén, University of Jaen, Campus Las Lagunillas s/n, 23071 Jaen, Spain*

[2]*Department of Electronic Engineering and Automatics, EPS de Jaén, University of Jaen, Campus Las Lagunillas s/n, 23071 Jaen, Spain*

Abstract:

This work presents a fast and practical method to determine a characteristic function that predicts a local ground response of vertical ground heat exchangers (GHE) in a short term, which is mandatory when intermittent operation modes are modelled. It expands the use of a Thermal Response Test (TRT) that is recommended previous to the design of a borehole field into a vertical Ground Source Heat Pump (GSHP). These tests are used to provide some ground thermal characteristics, such as ground conductivity or borehole effective thermal resistance. The same device can also be used to measure the undisturbed ground temperature along depth. From the measurements, it has been determined a temperature response factor function that characterizes the ground behavior in a short term as a consequence of a heat pulse. This function is then included into a finite line-source model to simulate the average temperature of the fluid that flows into the borehole pipes along time. In order to validate this method, several additional tests have been performed by the same device used for TRT's, with intermittent operation modes. For each test, both experimental and simulated average fluid temperatures have been compared. Results present an excellent accuracy; thus, they demonstrate de effectiveness of the method, as well as other advantages: i) fast and accurate; ii) prevents high precomputing times; iii) several uncertainties from measurements disappear when it is used.

Keywords:

Ground thermal modelling; Ground Source Heat Pump (GSHP); ground heat exchanger (GHE); g-function; short-time g-function (STGF); Thermal Response Test (TRT); Undisturbed Ground Temperature Test (GTT)

Nomenclature

a	Constant (ºC) of aggregated terms in ILS equation depending on ln(τ)
C_S	Ground volumetric heat capacity ($J \cdot m^{-3} \cdot K^{-1}$)
E_i	Exponential integral function (dimensionless)
H	Well depth (m)
m	Slope ($ºC \cdot s^{-1}$) in ILS equation depending on ln(τ)
q	Unitary Heat pulse ($W \cdot m^{-1}$)
q_i	Unitary Heat pulse, being i the end of a time step ($W \cdot m^{-1}$)

* Corresponding author
E-mail address: fcruz@ujaen.es

39	q_0	Unitary heat pulse injected in a TRT ($W \cdot m^{-1}$)
40	Q	Heat rate pulse (W)
41	r	Radius (m)
42	r_b	Borehole radius (m)
43	r_{dim}	Dimensionless radius, equal to r/H
44	R_b	Effective thermal resistance of the borehole ($K \cdot m \cdot W^{-1}$)
45	R_{b0}	Effective thermal resistance of the borehole from data of a TRT ($K \cdot m \cdot W^{-1}$)
46	T	Arbitrary temperature (ºC)
47	T_b	Borehole wall temperature (ºC)
48	T_f	Average fluid temperature (ºC)
49	T_{f0}	Average fluid temperature from measurements of a TRT (ºC)
50	$T_{f,\ measured}$	Average fluid temperature from measurements of a certain test (ºC)
51	$T_{f,\ modelled}$	Average fluid temperature modelled from ***g-function*** (ºC)
52	T_r	Ground temperature at radius 'r' (ºC)
53	T_S	Average undisturbed ground temperature (ºC)
54	T_{S0}	Average undisturbed ground temperature from measurements of a GTT (ºC)
55	**Greeks**	
56	α_S	Ground thermal diffusivity ($m^2 \cdot s^{-1}$) obtained from measurements of a TRT
57	γ	Euler's constant (dimensionless), equal to 0.5772156649
58	$\Delta T_{b,I}$	Rise of temperature at borehole wall in relation with T_S (ºC)
59	$\Delta\tau$	Interval time of on-off cycles of heat pulses (s)
60	ε_f	Deviation error $T_{f,\ measured}$- $T_{f,\ modelled}$ (ºC)
61	λ_S	Soil thermal conductivity ($W \cdot m^{-1} \cdot K^{-1}$)
62	τ	Time (s)
63	τ_{dim}	Dimensionless time, equal to τ/τ_S
64	τ_S	Time constant (s)
65	**Abbreviations**	
66	***DST***	Duct Ground Heat Storage model
67	***ECU***	Electronic Control Unit
68	***FLS***	Finite-line source model
69	***g-function***	Temperature response factor (dimensionless)
70	***GHE***	Ground Heat Exchanger
71	***GHG***	Greenhouse gasses emissions
72	***GSHP***	Ground Source Heat Pump
73	***GTT***	Undisturbed Ground Temperature Test
74	***ICS***	Infinite-cylindrical source model
75	***ILS***	Infinite-line source model
76	***LTGF, g_{LTGF}***	Long-Term g-function

PE	Parameter Estimation
PID	Proportional-Integral-Derivative regulation algorithm
PWM	Pulse-Width Modulation
STGF, g_{STGF}	Short-Term g-function
TRT	Thermal Response Test
VFD	Variable Frequency Drive

1. Introduction

Energy consumption in the building sector represents 40% of the global demands, being also responsible for, at least, on-third of the worldwide greenhouse gasses emissions (GHG) [1], where the cooling and heating equipment is the biggest consumer in them. The current global warming fosters the development of those energy-saving technologies for the reduction of carbon dioxide emissions as much as possible. In this sense, ground source heat pump (GSHP) is a current well-known technology that reaches both high savings of energy and GHG, being considered as an attractive renewable source. Its benefits have caused rapid development of this kind of installations, gradually increasing over time around the world, and maintaining this trend in the future [2-5]. The ground heat exchanger (GHE) corresponds to the external element of a GSHP, which exchanges heat with the soil. Among the several types of GHE, vertical disposition ones have been widely used in GSHP systems. Although the installation costs of vertical GHEs are higher than for horizontal ones, they present a smaller area and greater efficiency [6,7].

It is well known that the performance of vertical GHEs is reduced over time due to the accumulation of heat in the ground surrounding the borehole. Research in recent last years has demonstrated (in both numerical and experimental ways) that intermittent heat transfer for short-term operation in this kind of elements has a considerable influence on system effectiveness, especially with short cycles. When operation mode becomes discontinuous in reduced periods of time, this partly relieves heat accumulation, improving its performance consequently [8]. It has also been demonstrated that an intermittent process improves the use of the ground energy, approaching to an ideal heat pump working condition, at a temperature lower in the condenser or higher in the evaporator of the GSHP system [9]. Among other analyses, Choi et al. [6] evaluated the influence of unsaturated soil conditions applied to intermittent operation of a GHE, concluding the increasing of its performance in relation to continuous mode. Miyara and co-workers [7] evaluated different operation modes in several types of vertical GHEs. They also demonstrated that intermittent operation increases the heat exchange rate. For example, a discontinuous 2 hours operation in cooling mode supposes an increase of the minimum heat exchange rate of 17.1% for a U-tube, increasing it up to 32.6% for 6 hours operation mode. It was demonstrated the improvement of the performance, and the possibility of reducing the borehole depth of the GHEs. Summarizing these previous works, it has been reported that the heat flux transferred is higher, as well as the average temperature of the fluid in the tubes can be lower, avoiding soil saturation. Discontinuous flow into the borehole focuses on the best behavior of the GSHP, providing maximum productivity, which joins the dynamics of both the well and the ground,

undergoing continuous changes in their temperatures. The intermittent time intervals, heat exchange loads and periods of previous operation are key factors to be taken into account to improve all the arrangement. In any case, in order to find an optimal solution, it is necessary to use as reliable models as possible, allowing to reduce the size of the system in a design stage.

Detailed information about vertical GHE models and software can be reviewed [10]. Long-term models were developed based on the Kelvin's line-source theory, which have been improved over time. Most of them are based on a temperature response factor, called ***g-function*** [11] developed and used into the finite line-source method (FLS). Initially, it is only valid for a certain number of hours, where the heat transfer through the well can be considered as in a steady-state, so it is also called long-term ***g-function*** (LTGF). It has reached a very widespread and sufficiently validated use to model a long-term behavior of a GSHP.

However, the intermittent behavior of a GSHP presents significant differences that can not be evaluated with long-term models [8,12], being more pronounced for cooling demands [13]. To improve the accuracy of the actual GHE behavior in short periods of time, several analytical, semi-analytical, numerical and lumped element models have been conducted, where the borehole thermal capacity has been taken into account [6,14-19]. They afford a better understanding of the whole heat exchange in GHEs, to be applied for design and optimization purposes in GSHP systems. Most of them are associated with the extension of Eskilson's work about a temperature factor for a shorter scale, called short-time ***g-function*** (STGF), obtained firstly from synthetic data produced by a 2D numerical model [20]. These functions, next to several improvements, have been included in several designing software tools, modeling any heat pulse over any time interval [21]. Alternative progress from this approach can also be found nowadays, such as from Brussieux and Bernier [18], where the synthetic data for calculating the short-time g-function were yielded by a hybrid approach: heat transfer from the fluid to the borehole wall was evaluated by a finite volume based numerical method, while the corresponding one from that wall towards the ground was calculated analytically using the infinite cylindrical heat source model (ICS). A recent work has also been developed in order to construct these STGFs using artificial neural networks [19] where the necessary temperature data came from a lumped model [15].

Depending on the source, the most significant transient effects occur during the first 3 to 12 hours [7,22], and since then, trends approach to that long-term behavior, which could be set between 50 [14] and 200 hours [20]. According to this feature, this time range contains a common point where both LTGF and STGF converge.

Although satisfactory results have been got, the researchers agree that the validity of the simulations should be verified, requiring greater development than results in a short-term GHE model that might be reliable, friendly and fast. In addition, its integration into a design or control procedure requires a previous preprocessing work to result in the different functions that will be used later. Thus, the computational load associated with this first step is usually high.

In any case, it is mandatory the knowledge of several ground and borehole thermal characteristics, which are unknown a priori for the design of a GSHP system at a particular location. In this sense, an accepted and widespread method for determining ground properties

consists of an in-situ test into one vertical GHE: Thermal Response Test (TRT) [23]. Data collected form this TRT serve to calculate both the soil thermal conductivity λ_S and the effective thermal resistance of the borehole R_b usually by means of the infinite line-source model (ILS) [24,25]. A test of 3 to 4 days is recommended (between 72 and 96 hours). Moreover, it is also required the mean undisturbed ground temperature T_S, which can be determined carrying out a previous ground temperature test (GTT), using the same device as for the TRT [26].

Several uncertainties appear associated with the test running and parameter estimation (PE), due to characteristics of the different elements of the experimental device as well as ambient conditions [24,27,28]. Special care must be taken with the processing of data to provide adequate values of the required features [29]. In this sense, Zhang et al. [30] compared the ILS method with other ones, to determine those thermal characteristics from TRT data, and their impact on the design length of a borehole heat exchanger: infinite cylindrical source model (ICS), several ones based on the finite line source model (FLS), and the duct heat storage model (DST). They have been used several parameter estimation procedures (PE) based on the least-squares minimization method to solve the inverse heat conduction problem. They found a considerable difference between the estimated values depending on the used method, such as a 34.4% for the borehole thermal resistance, or 11.9% for soil thermal conductivity, translating uncertainties for computing the borehole design length, causing about a 15% relative difference in the very beginning and 5% at the end of the simulation periods in relation with the fluid temperatures. They concluded that simple equation-based methods seem not to be as adequate as they might for design purposes. But in contrast, when the simplest of them (ILS) is used to PE, their results match quite well when another improved method (such as software-based or complex analytical functions) is used for a GHE design, with differences below 5% of the final borehole design length.

From this background, several points can be highlighted: i) the determination of soil characteristics from a TRT can use the ILS model with high reliability, which infers the average temperature of the fluid T_f; ii) on the other hand, the FLS equation, where the ***g-function*** is included, considers the radial-axial effects of heat transfer, evaluating the temperature at any point located at a distance of radius r from the center of the well. The perforation wall requires special attention, with temperature T_b and known radius r_b. With this approach, the T_f can also be determined by including in the equation the effective resistance R_b of the elements included inside the borehole (fluid, pipes and filling material, such as bentonite). From this point of view, the result of the FLS model must match that one from the ILS equation, at least in a small time interval of the test; iii) the time intervals associated with a TRT (72-94 hours) and an STGF (50-200 hours) turn out to be quite similar.

With all these premises in mind, it is possible to launch the hypothesis that a TRT can be used to supply a local STGF that serves to model the behavior of a GHE in the short term, especially with intermittent heat rate cycles. Until now, ***g-functions*** have been derived from synthetic data, which requires a considerable previous time. An experiment-based STGF could remove this disadvantage completely.

The aim of this work is to evaluate the goodness of the use of a local STGF based on experiments, to simulate the behavior of a vertical GHE in short intervals of time, with high reliability. Its determination also needs a low computing charge. For this purpose, both an undisturbed ground temperature test (GTT) and a thermal response test (TRT) have been carried out in a single vertical borehole, determining first the thermal characteristics associated with it. These ones, together with the real evolution of the average fluid temperature T_f, use the FLS model to establish the profile of a STGF, following the same procedure presented by Yavuzturk [20]. The difference is that here the experimental temperatures of the fluid are used to generate that function. To validate the methodology, a set of different short cycles tests has been developed, for which it has been necessary to reprogram the TRT device, measuring fluid temperatures. Their values have also been modeled from that STGF and compared.

All the contributions of this work will serve to promote the use of experimental data from a TRT to provide that local STGF curve. It contains all the information about a GHE characterization for design and optimization purposes, avoiding the use of a precomputed previous one in other ways that not always could assure enough accuracy.

2. Material and methods

2.1.- Experimental set-up

Figure 1 shows the set-up proposed for the done work [31]. A basic scheme of the device is presented, where a centrifugal pump makes the transference fluid to circulate along the U-tube into the borehole. This fluid is heated by an electrical resistance immersed in a small tank. A 3-paths valve makes the fluid to pass across the tank or not, depending on the kind of test performed. Temperature sensors at inlet and outlet ports (PT-100, range 0ºC-50ºC, ± 0,5ºC accuracy), as well as an ultrasonic volumetric flow meter (range 0,25 to 25 l/min, that is, from $4{,}17 \cdot 10^{-6}$ to $4{,}17 \cdot 10^{-4}$ m^3/s, accuracy ±3% accuracy), are required for measurements. Auxiliary elements have not been represented, in order to simplify that scheme, including among them the following: inlet and outlet pressure sensors (piezo-resistive type, range 0-1MPa, ± 0,003MPa accuracy), a filter for avoiding impurities, a check valve, an expansion tank, an overpressure valve, as well as pressure, flow and temperature switches.

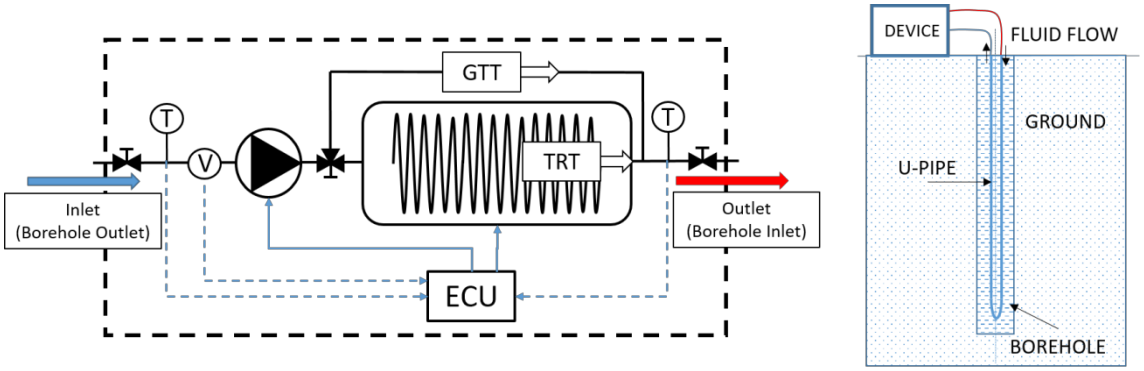

Figure 1. Experimental set-up

The electronic control unit (ECU) drives both the pump and resistance, in order to reach both the pre-defined volumetric flow rate and inlet temperature to the tube (to assure a constant heat pulse) that the corresponding test requires, also using security switches if it is necessary. A

variable frequency drive (VFD) is connected to the pump, varying the volumetric flow rate according to test specifications. Moreover, a solid-state relay acts over the tank resistance by means of pulse-width modulation (PWM). Both actuators are directed by PID (proportional-integral-derivative) regulation algorithms, implemented in the ECU. Apart from the ability to carry out the conventional tests (TRT and GTT), changing heat pulses, periods and volumetric flow rate, the flexibility of the designed device allows defining other ones, such as intermittent cycles.

A single borehole located at the University of Jaén completes this set-up: a single U-tube (36mm inner diameter, 2mm thickness, polyethylene PE 100 SNR11 PN-16) is immersed into a vertical well of 130m deep, 150mm diameter, filled with bentonite.

The first test measures the unaltered ground temperature in depth (GTT): with the device off, the circuit is connected and filled with the transfer fluid. Later, it is necessary to wait a few days to stabilize its temperature that reaches the same value as the ground. Then, the pump starts circulating the fluid into a laminar regime to avoid heat losses during its path. The temperature of the fluid at every moment is measured in the inlet sensor of the device (tube outlet), which corresponds to a particular ground temperature associated with a certain depth. In this test, the resistance remains off [32]. The required test time varies, depending on the borehole depth, between 10 and 30 minutes.

Later, for the TRT [24,33], the ECU controls both the pump and the resistance using the different sensors, in order to adjust the rates of volumetric flow and heat in the test, whose values must be defined previously and must be constant throughout the proof. It lasts between three and four days, being that period of time also defined by the user. The reliability of the results must be ensured by assessing uncertainties of all measured data (pressures, temperatures, heat rate and volumetric flow). These uncertainties can be mainly associated to the inherent characteristics of sensors, data acquisition, calibration of the measurement system, and power supply conditions [27].

2.2.- Thermal properties determination based on TRT

For a given unitary heat pulse $\boldsymbol{q}$ (W/m), obtained by dividing the heat pulse $\boldsymbol{Q}$ (W) into the borehole depth $\boldsymbol{H}$ (m), the infinite line-source (ILS) model relates the measured average fluid temperature $\boldsymbol{T_f}$ (ºC) into a GHE along the time $\boldsymbol{\tau}$ (hours) following the next expression [24]

$$T_f = T_S + q\,R_b + \frac{q}{4\,\pi\,\lambda_S}\,E_i \approx T_S + q\,R_b + \frac{q}{4\,\pi\,\lambda_S}\left[\ln\left(\frac{4\,\alpha_S \tau}{r_b^2}\right) - \gamma\right] \quad (1.a)$$

$$T_f = a + m\ln(\tau) \quad ; \quad m = \frac{q}{4\,\pi\,\lambda_s} \quad ; \quad a = T_S + q\,R_b + \frac{q}{4\,\pi\,\lambda_S}\left[\ln\left(\frac{4\,\alpha_s}{r_b^2}\right) - \gamma\right] \quad (1.b)$$

where $\boldsymbol{r_b}$ (m) is the borehole radius; the soil thermal conductivity and diffusivity are denoted by $\boldsymbol{\lambda_S}$ (W/mK) and $\boldsymbol{\alpha_S}$ (m^2/s), respectively; $\boldsymbol{T_S}$ (ºC) corresponds to the mean undisturbed ground temperature far from the GHE; $\boldsymbol{R_b}$ (m K/W) is the effective steady-state borehole thermal resistance [34], and $\boldsymbol{E_i}$ is the exponential integral function [35], that can be simplified, as eq. (1.a) shows, that includes the Euler's constant $\boldsymbol{\gamma}$. As a constant heat pulse is maintained along the test, this expression takes a linear tendency depending of the natural logarithm of time.

The method for $\boldsymbol{\lambda_S}$ estimation starts with plotting $\boldsymbol{T_f}$ along that natural logarithm of time. The late-time of it follows a linear trend, as eq. (1.b) depicts, being the soil thermal conductivity

inversely proportional to its slope ***m***. It must be noted that the estimation of $\boldsymbol{\lambda_S}$ is not sensitive to the choice of using the mean temperature approximation instead of any of both extreme measured ones, because the late-time slopes are all the same [25]. Besides, providing previously the soil volumetric heat capacity $\boldsymbol{C_S}$ (MJ/m^{3}K) from tables, the soil diffusivity $\boldsymbol{\alpha_S}$ (m^2/s) can be determined by means of the relation $\alpha_S = \lambda_S / C_S$. The use from tables, instead of determining it by other experimental way, may include some uncertainty in the final results, although with low importance. The constant ***a*** includes $\boldsymbol{R_b}$ and $\boldsymbol{\alpha_S}$, correlating them directly. As a consequence, the borehole resistance $\boldsymbol{R_b}$ can be straight determined from that [24,25]. In this case, higher uncertainty can appear. For more accurate results in this term, it is better using p-linear average (with p tends to -1) for $\boldsymbol{T_f}$, instead of the arithmetic average of extreme fluid temperatures into the U-tube [29].

It is important to remark that the procedure neglects the major of the data in order to find the slope ***m*** at the end of the test, and so, determining $\boldsymbol{\lambda_S}$. There is a large amount of information that is discarded, being associated with the first time interval of a heat rate step, which is very wide, where transient effects are very pronounced. They can be directly associated to a short-time behavior that might be taken in advantage.

2.3.- Extending capability of TRT measurements for determining an experimental based STGF

With the finite line-source model (FLS), the temperature response to a step heating ***q*** (W/m) in a single borehole over a point at a radial distance ***r*** from its center and time ***τ*** corresponds to a ***g-function***, that expresses the excess of temperature ***T*** at that point in relation with the undisturbed one $\boldsymbol{T_S}$ as eq. (2) shows [11]:

$$g(\tau_{dim}, r_{dim}) = \frac{2\,\pi\,\lambda_S}{q}\;(T - T_s)\,; \quad \tau_{dim} = \frac{\tau}{\tau_S}\,; \quad r_{dim} = \frac{r}{H} \qquad (2)$$

for a given steady-state time $\tau_s = H^2/9\cdot\alpha_S$, thus $\tau_{dim} = 9\cdot\alpha_S\cdot\tau/H^2$. This function was first computed numerically. Later, an analytical solution was performed [36] for determining that function, using a $\tau_{dim} = \alpha_S\cdot\tau/H^2$, thus implying $\tau_s = H^2/\alpha_S$, reducing considerably precomputing times. In any case, relations for this temperature response factor are acceptable for a long term point of view, only valid for times higher than $5\cdot r_b^2/\alpha_S$ (it implies from 3 to 6 hours). This function has a particular importance for the temperature at the wall borehole $\boldsymbol{T_b}$, with radius $\boldsymbol{r_b}$: as the heat transfer across the grout material can be considered as steady-state on a long term, $\boldsymbol{T_b}$ and $\boldsymbol{T_f}$ are related by means of the product of $\boldsymbol{R_b}$ and ***q***, thus:

$$T_f = T_S + q\,R_b + \frac{q}{2\,\pi\,\lambda_S}\,g(\tau_{dim}, r_{dim}) \qquad (3)$$

Yavuzturk and Spitler [20] prolonged the previous method to develop an STGF approach. For this purpose, a 2D numerical model was used in a well with single U [37], known as its geometry, $\boldsymbol{\lambda_S}$ and $\boldsymbol{R_b}$ (implicit discretization of finite volume in a polar grid) determining the average temperature of the fluid in the tube over time $\boldsymbol{T_{f0}}$, from a step of unitary heat flow rate $\boldsymbol{q_0}$. The results were validated by comparing it with known analytical approach. This method was included as a component model in commercial software to model GSHP systems. In any case, the authors commented that a comprehensive experimental validation would be useful.

As a consequence, eqs. (2) and (3) were reformulated, presenting the ***g-function*** the following expression:

$$g(\tau_{dim}, r_{dim}) = \frac{2\,\pi\,\lambda_S}{q_0}\,\left(T_{f0} - T_{S0} + q_0\,R_{b0}\right) \quad (4)$$

As a result of this, a ***g-function*** can be precomputed for any time in a single borehole. In order to establish a design composed of several boreholes, a complete ***g-function*** must then be determined, also. It serves to design and optimize a GHE into a GSHP without using complex models nor simulations. It is necessary to differentiate between STGF and LTGF. Figure 2 presents an example of this function, for a single borehole and for a 3x3 squared GHE configuration (6m separation between boreholes; $\boldsymbol{\alpha_S}$ =1.6e-6 m^2/s; $\boldsymbol{r_b/H}$ = 6.25·10^{-4}). In the first time interval, both profiles are the same.

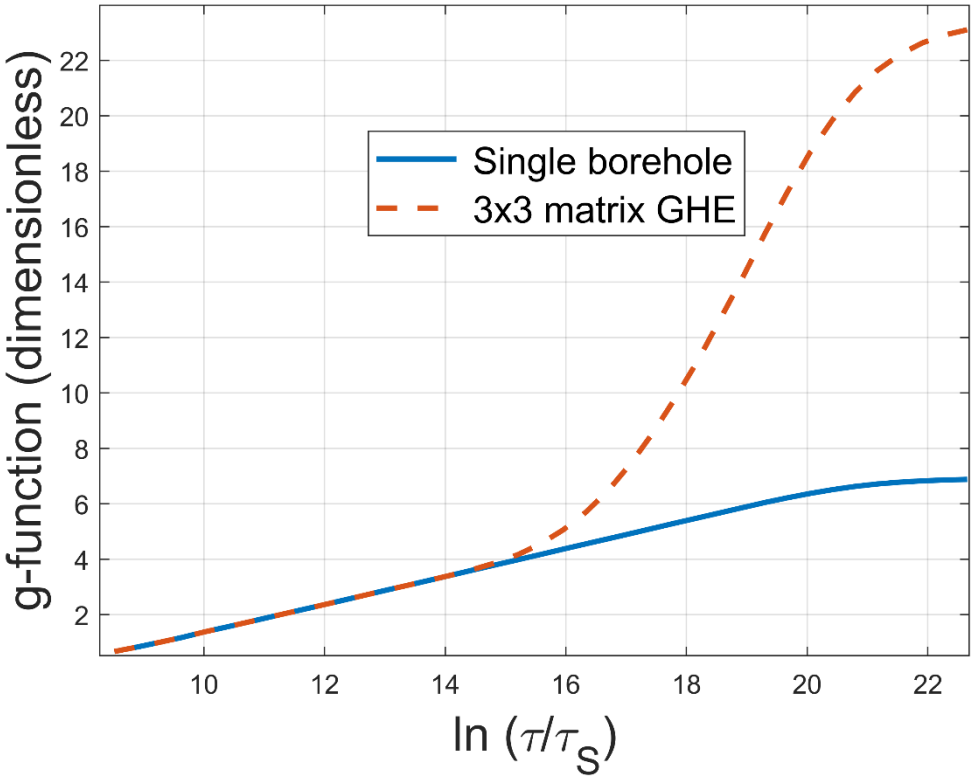

Figure 2. Example of ***g-function*** representation for a certain 3x3 configuration GHE

When eqs. (1) and (4) are compared, the following equality appears:

$$g(\tau_{dim}, r_{dim}) = \frac{1}{2}\,E_i \quad (5)$$

It implies that the ***g-function*** must follow the trend of this curve, for a given set of necessary data, such as $\boldsymbol{\lambda_S}$, $\boldsymbol{r_b}$, and $\boldsymbol{\alpha_S}$. Discrepancies between infinite and finite line-source models can be found in Marcotte et al. [38] although this analysis was performed for a long-term point of view. The exponential integral is fundamental in the first one, since it is reliable for times greater than $20 \cdot r_b^2/\alpha_S$, but does not consider the axial effects. Otherwise, the analytical approach [36] provides acceptable values for times higher than $5 \cdot r_b^2/\alpha_S$. Differences increase with the Fourier's number ($\boldsymbol{\alpha_S \cdot \tau / r^2}$), thus the longer the time, the higher the dissimilarities appear. As this work is focused on short-term behavior, the differences must be very small in both the response temperature factor and average temperatures, at least in a short time interval at the end of the test. If other expressions are used to determine the ground thermal characteristics, such as those

extracted from ICL or DST methods, they all have this common point: both the ***g-function*** and T_f must be quite similar, at least in a little time interval (which might be higher than for the case in which the ILS equation is solved).

Another point of view can be applied as a result of accommodating eqs. (3) and (4) for a single borehole. The average fluid T_f evolution from an arbitrary heat step q can be modelled taking into account the original values used for the established ***g-function***, denoting the high influence of three terms: q, R_b and T_s, which can be related as follows:

$$T_f = \left[1 - \frac{q}{q_0}\right] T_{S0} + q(R_b - R_{b0}) + \frac{q}{q_0} T_{f0} \quad (6)$$

There is an initial transient behavior into the grout that this method seems to ignore, appearing an implicit mistake associated both terms R_{b0} and R_b. Dissimilarities between them are only due to the convection coefficient fluid-pipe inner wall, that mainly varies due to the fluid speed, associated to the volumetric flow rate [39] , presenting a very low influence in the borehole resistance estimation. Thus the same value can be considered for both the terms, disappearing the possible initial estimation error, and minimizing or removing the second component in eq. (6), even for those cases in which R_b and R_{b0} could be considered as variable over time.

Into the bargain, T_{s0} effect on the temperature estimation is proportional to the term ($1-q/q_0$), being very low for similar values in both q and q_0. Designers' experience allows them to specify reliable heat rate values for a given configuration into a GSHP design. Therefore, the initial establishment of q_0 for deriving a STGF can take analogous values to those that will eventually be included in the GHE model.

As a result of this, it can be observed that for a given heat step pulse, the model practically reproduces T_{f0} multiplied by the ratio q/q_0. It means that the STGF contains all the necessary information about de thermal transient behavior of the entire set, including fluid, pipes, filling material and ground.

A TRT presents several similarities to use its data as a basis for providing a local STGF: i) it includes a calorific flow step to set q_0; ii) extreme fluid temperatures are measured, from which evaluate the average value T_{f0} along the test; iii) both λ_S and R_{b0} can be extracted from the exposed method through the infinite line-source model (ILS); iv) the test time interval resembles that needed of a STGF. Furthermore, if a GTT is previously carried out, the unaltered ground temperature T_{s0} can also be known. Therefore, eq. (4) can be solved as a result of the data processing from these tests.

2.4.- Applicability

The principle of superimposition in space is employed to consider the temperature responses for multiple boreholes. In a GHE with I number of them, the rise of temperature on the wall of the borehole concerned $\Delta T_{b,i}$ (with radius r_b) at time τ due to a constant heat step q_i can be evaluated as eq. (7) shows:

$$\Delta T_{b,i} = \frac{q}{2\,\pi\,\lambda_S}\left\{g_{LTGF}\left(\tau_{dim}, \frac{r_b}{H}\right) + \sum_{j=1}^{l-1} g_{LTGF}\left(\tau_{dim}, \frac{r_j}{H}\right)\right\} = \frac{q}{2\,\pi\,\lambda_S}\, g_{LTGF,\ GHE}(\tau_{dim}) \quad (7)$$

$$g_{LTGF,\ GHE}(\tau_{dim}) = \frac{q}{2\,\pi\,\lambda_S}\left\{g_{LTGF}\left(\tau_{dim}, \frac{r_b}{H}\right) + \sum_{j=1}^{l-1} g_{LTGF}\left(\tau_{dim}, \frac{r_j}{H}\right)\right\}$$

Additionally, the sequential temporal superimposition in time also serves to evaluate the temperature response to any arbitrary heat rate, which can be decomposed into a set of n single step pulses q_i, each one starting at time τ_{i-1}, being i the end of a time step. For a composed borehole and long term, this rise ΔT_b will be [40]:

$$\Delta T_b = \sum_{i=1}^{n} \Delta T_{b,i} = \frac{1}{2\,\pi\,\lambda_S} \sum_{i=1}^{n} \left\{ (q_i - q_{i-1})\, g_{LTGF,\ GHE}\left(\frac{\tau-\tau_{i-1}}{\tau_s}\right)\right\} \quad (8)$$

All these features were firstly developed for LTGF, where interactions between the different components into a borehole field are significant. For shorter periods (a few hours) those interplays don't exist. If an intermittent heat transfer is wanted to be evaluated into a borehole from a starting time τ_0, it is necessary to take into account previous loads. For this purpose, a load aggregation scheme is required to calculate the current temperature, which decreases progressively as it goes back in time [22]. All the loads along time can be decomposed into a set of long-term heat step pulses and a sequence of short time ones. The first long-term set establishes the conditions of the borehole wall at the starting time for evaluating the following short time period.

From eqs. (3) (4), (7) and (8), and taking into account the load aggregation, differentiating long and short terms, and experimental known data from GTT and TRT, values for $T_f(\tau)$ for a certain borehole into a composed field can be modelled for an arbitrary heat released $q(\tau)$, once decomposed in n long term step pulses and k short term ones, as follows:

$$T_f = T_{S0} + \frac{1}{2\,\pi\,\lambda_S} \sum_{i=1}^{n} \left\{ (q_i - q_{i-1})\, g_{LTGF,\ GHE}\left(\frac{\tau-\tau_{i-1}}{\tau_s}\right)\right\} + R_{b0} \sum_{i=1}^{n} (q_i - q_{i-1})$$

$$+ \frac{1}{2\,\pi\,\lambda_S} \sum_{j=1}^{k} \left\{ (q_j - q_{j-1})\, g_{STGF}\left(\frac{\tau-\tau_{j-1}}{\tau_s}\right)\right\} + R_{b0} \sum_{j=1}^{k} (q_j - q_{j-1}) \quad (9)$$

Figure 3 shows a graphic example where an intermittent operation is required to be analyzed starting at time τ_0. However, it is after two additional injection periods, both of them separated in time, considering their influence in the long term. Its temperature profile $T_b(t)$ is shown in the upper curve, which parts from an undisturbed soil temperature T_s, evolving as a result of different heat rates $q_i(t)$ that the graphic in the figure center shows. During the first preceding period, a constant unit heat rate q_1 is injected, thus T_b is increased. After that, temperature diminishes while the storage heat is diffused across the soil. In the second injection period, an intermittent behavior is carried out. Although there are several oscillations around the both average heat and temperature profiles (presented with dash lines), they disappear a little time after finishing that interval. Thus, a mean value for the heat rate q_2 is enough to evaluate its influence for a long term in the third period. These heat rates can be decomposed into several heat step pulses, such as the bottom profile shows, and their long term influence must be included during the analysis of the current intermittent period (third time interval in the figure), taking into account the LTGF. Furthermore, the current heat pulses in it must be also decomposed into several heat steps, but in this case, the STGF will be used to model the thermal response, for a single borehole.

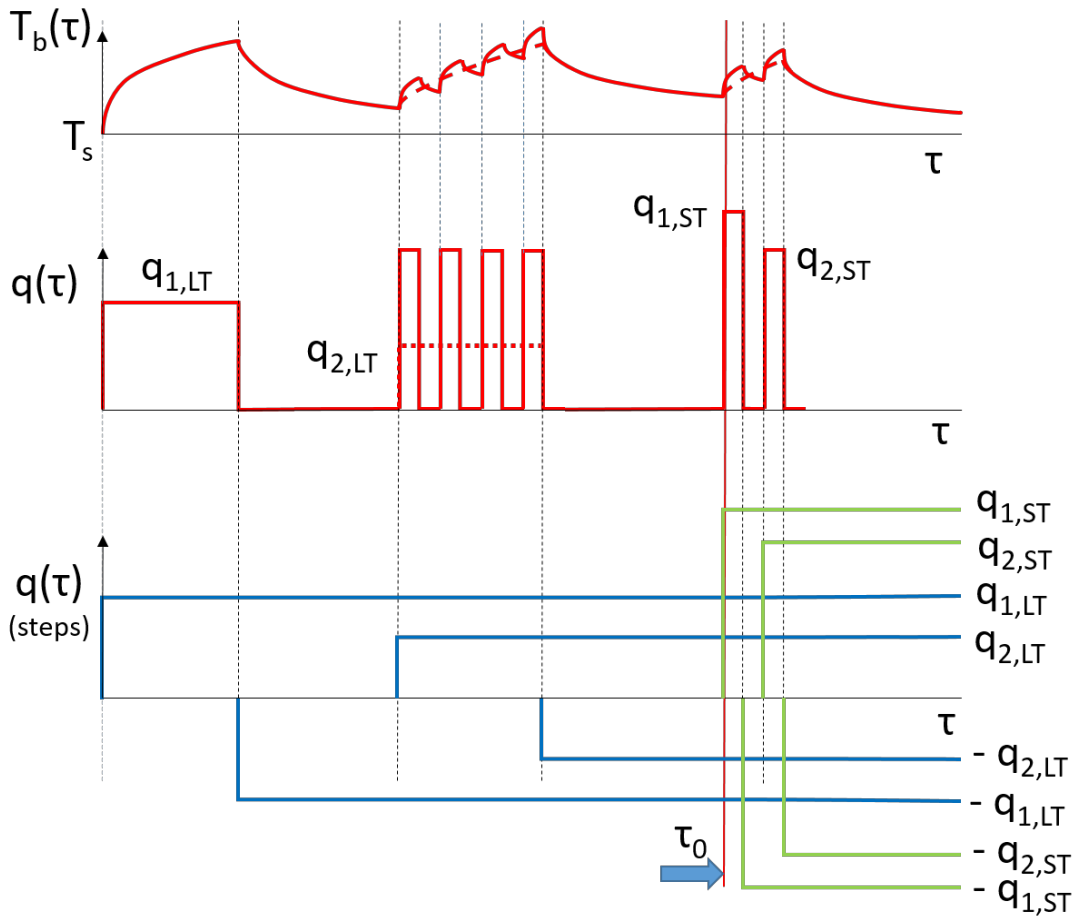

Figure 3. Example of loads aggregation to model a GHE

2.5. Validation procedure

After finishing the GTT, the TRT will be performed specifying both the volumetric flow and the heat rate. Average fluid temperature evaluated from measurements will serve to determine λ_S, R_{b0}, and then, the STGF profile. This curve will be attached to a LTGF profile in a long term, calculated following the analytical approach [36], thus providing a complete ***g-function*** similar to that showed in Fig. 2. Then, several intermittent tests for different volumetric flow rates, heat rate pulses, and time intervals, will be run. For each test, simulations will be done following eq. (9), and later, their results will be compared with the experimental ones. In this sense, dates of all the tests must be taken into consideration, in order to establish an adequate sequence of previous heat steps to each intermittent proof. They will be considered as long-term components into the total aggregated load, as it has been previously explained.

3. Results and discussion

3.1.- Initial test and thermal characteristics determination

First, the undisturbed ground temperature test along depth was done (GTT, as well as the thermal response test of the ground (TRT), for mean values of 15l/min ($2.5 \cdot 10^{-4}$ m^3/s) volumetric flow rate and 4000W heat rate. Following the procedure from Sharqawy [27], total uncertainties of ±0.5ºC in measured temperatures (at inlet and outlet ports, as well as for T_f), ±0.003MPa in measured pressures (differences between inlet and outlet port that start with

0,08MPa up to 0,02MPa at the end of the TRT), and 3% for flow metering, are initially estimated (including sensor, data acquisition and calibration uncertainties provided by the manufacturers)

In addition, results of fluid flow metering and heat rate present discrete probability density functions, as Fig. 4 shows, that can be fitted to analytical normal probability distributions with very little deviations: a 1.5% standard deviation has been observed for measures of the volumetric flow, as well as 2.8% maximum oscillations around the mean value into a 95% confidence level; regarding to the heat rate, results showed a 2% standard deviation, and variation up to 4% into a 95% confidence level. It demonstrates that the control procedure provides constant values of those parameters during the test.

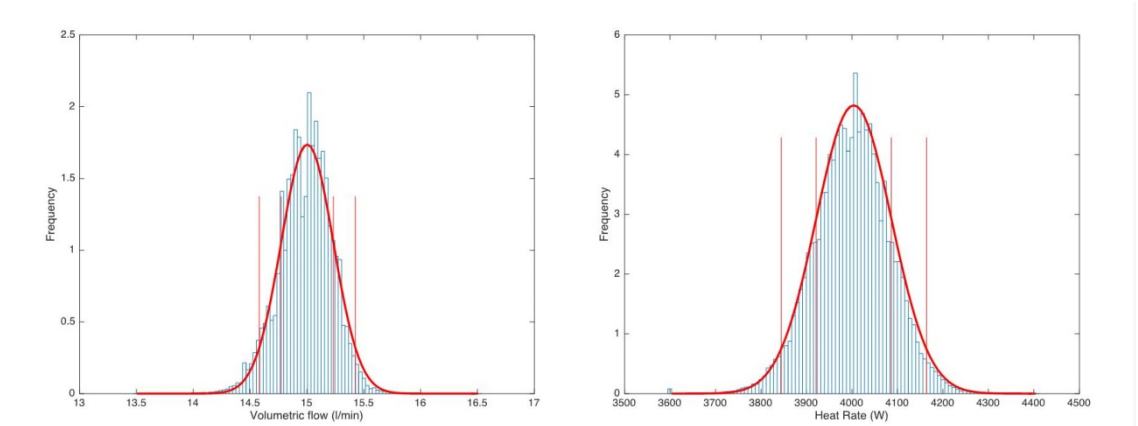

Figure 4. Histograms for volumetric flow and heat rate along the TRT

Once considered last tasks, results for both tests can be seen in Fig. 5.

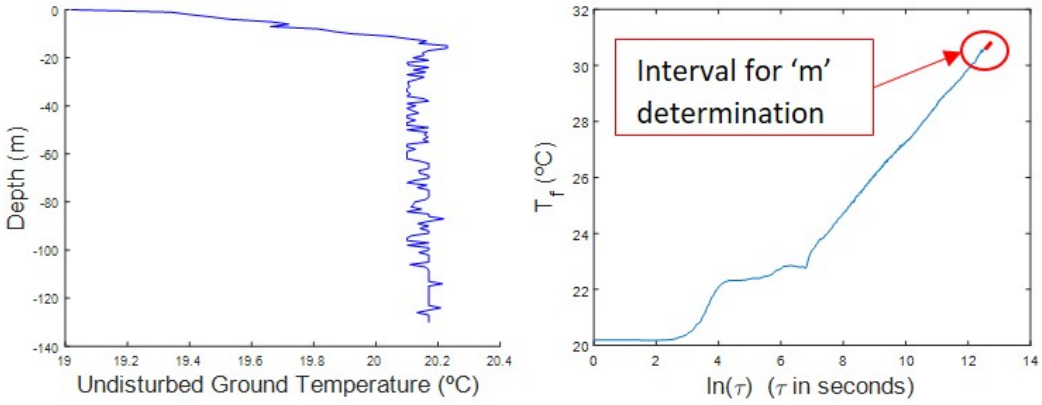

Figure 5. GTT and TRT results

The average soil temperature T_{s0} is 20.15ºC. Then, representing results of the TRT respect to the logarithmic time (see Fig. 5), and focusing in the last period, the slope m can be inferred, and from this, a λ_S of 1.88 W/mK. Later, once extracted from tables a C_S value of $2.2 \cdot 10^6$ J/m^{3}K [41], it gives a α_S of $8.6 \cdot 10^{-7}$ m^2/s. Finally, R_{b0} is calculated from the constant a in eq. (1.b), with a result of 0.141 m·K/W.

The next step consists of determining the STGF profile by solving eq. (4) that can be seen in Fig. 6. It has been also presented an approach of it based on the exponential integral, as eq. (5) indicates, as well as the analytical LTGF for those thermal and geometric characteristics. All of them are presented depending on the direct time as they have been evaluated starting from a

time zero and for that local and a specific use. In order to maintain the experimental nature of the procedure, results have not been filtered, as well.

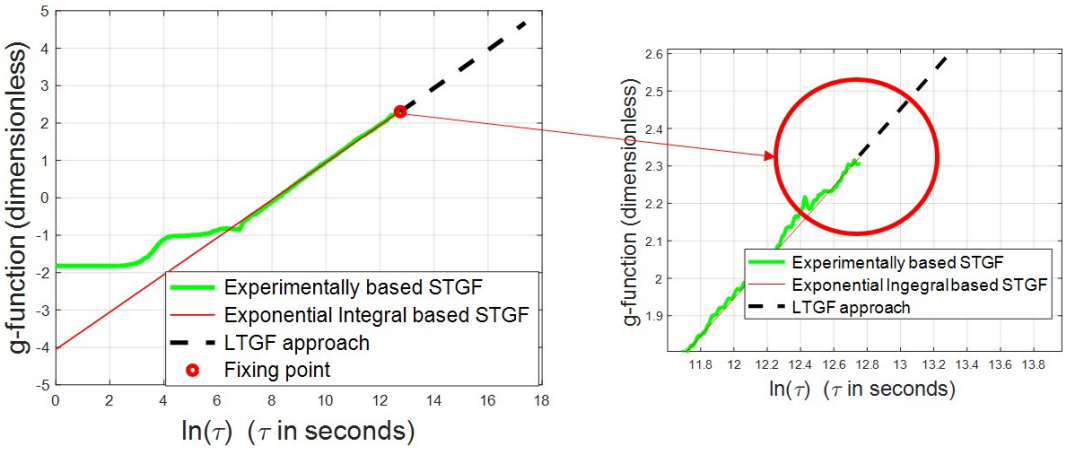

Figure 6. Temperature response factors

Some interesting points can be observed: i) as the thermal characteristics have been extracted from the infinite line-source model, and later, the STGF have been derived using them, both STGF curves the experimentally and exponential integral based, have the same slope and similar values in that period at the end of the TRT; ii) an initial negative error appears in a first interval of that curve. While R_{b0} is considered constant, it produces these negative values. In a formal way, they might not be admitted, but it only would be possible if a variable R_{b0} profile were depicted, taking into account capacity effects, so complementing that STGF curve into the model. In any case, for either constant or variable R_{b0}, its effects disappear as it was explained in a previous section, taking R_b logically the same value as R_{b0}; iii) it can be observed that at the end of the experimental period, both the STGF and the LTGF profiles are quite close. It means that the 96h time (end of this particular TRT) could be assumed as the connecting point between both curves, that can be attached in a unique profile to be used for simulations; iv) from the starting of the test, different jumps appear in the STGF profile as one new lap is closed by the fluid along its path. It takes less than 15 minutes for a fluid particle to make the round trip along the pipes circuit, for a given volumetric flow rate of 15l/min. During the first haul, no particle into the pipe suffers a significant variation in its temperature, maintaining a nearly constant value at the borehole outlet. A little step appears at the end of this first round: the diffusion effects take place for the fluid that has entered during that period, and then starts coming out from the tube. As complete loops come about, diffusion effects take more importance, so those leaps are more and more diminished. They take place at constant time intervals, depending on the desired volumetric flow rate. Thus, it is essential to evaluate the model results when values different than 15l/min are considered.

3.2.- Validation: additional experiments and model outputs

To validate the usefulness of this STGF, a set of additional tests have been carried out, whose main characteristics are presented in Table 1. It is important to remark the importance of the date for each experiment, because of the transient nature of the heat transferred across the ground. As the model considers a successive sequence of heat steps, all of them must be taken into account along the time (following the procedure summarized in fig. 3). When a certain

experiment is done, the injected heat is stored and diffused across the ground, disturbing the initial values of its temperatures at the beginning of the next proof.

Each experimental intermittent heat load has been applied by means of heat pulses with different duration, but for two tests, where it was variable. In any case, these loads have been precomputed for the model as a sequence of several heat steps. In all of them, "off" periods of heat pulses also imply that the fluid does not circulate. With the new STGF (see fig. 6), T_f is then modelled following eq. (9), for a single borehole, taking into account the aggregated loads which include previous heat steps, for both long (with average heat pulses known and time intervals) and short (in this case, associated to the current test) terms.

Table 1. Test set for validation

Test Nr.	Heat Pulse, W	Volumetric Flow rate, l/min [m^3/s]	$\Delta\tau$ periods on-off
1	6000	15 [$2.5 \cdot 10^{-4}$]	12h-12h
2	6000	15 [$2.5 \cdot 10^{-4}$]	15'-15'
3	Variable	15 [$2.5 \cdot 10^{-4}$]	6h-6h
4	5000	20 [$3.33 \cdot 10^{-4}$]	12h-12h
5	4500	20 [$3.33 \cdot 10^{-4}$]	10'-10'
6	Variable	20 [$3.33 \cdot 10^{-4}$]	6h

Fig. 7 shows an example of results for one intermittent test (nr. 1 in Table 1): in the top graphic in Fig. 7.a, appears the real heat rate along the test (that presents oscillations due to the real operation of the device) and its fitting to a sequence of constant heat pulses Q_j (W) that serve as input load profile to the model. In the centered graphic of this figure, average fluid temperature is shown, for both measured and modelled values. Here appears a limitation to be considered: when the fluid is at rest ("off" periods), and even at the initial moments where the fluid flows again ("on" periods), the extreme experimental temperatures are not representative for determining an average reliable value of T_f, because the internal diffusion of heat from the pipe changes its temperature profile. At these intervals, there is no sense in comparing results. Thus, the bottom curve in Fig. 7.a represents the deviation error ε_f (ºC) of these temperatures along the experiment ($\varepsilon_f = T_{f.measured} - T_{f,modelled}$). Values to asses are associated only to "on" periods (when the fluid circulates), neglecting those ones in the "off" intervals. As a result of this, Fig. 7.b shows a discrete density function of this estimation error.

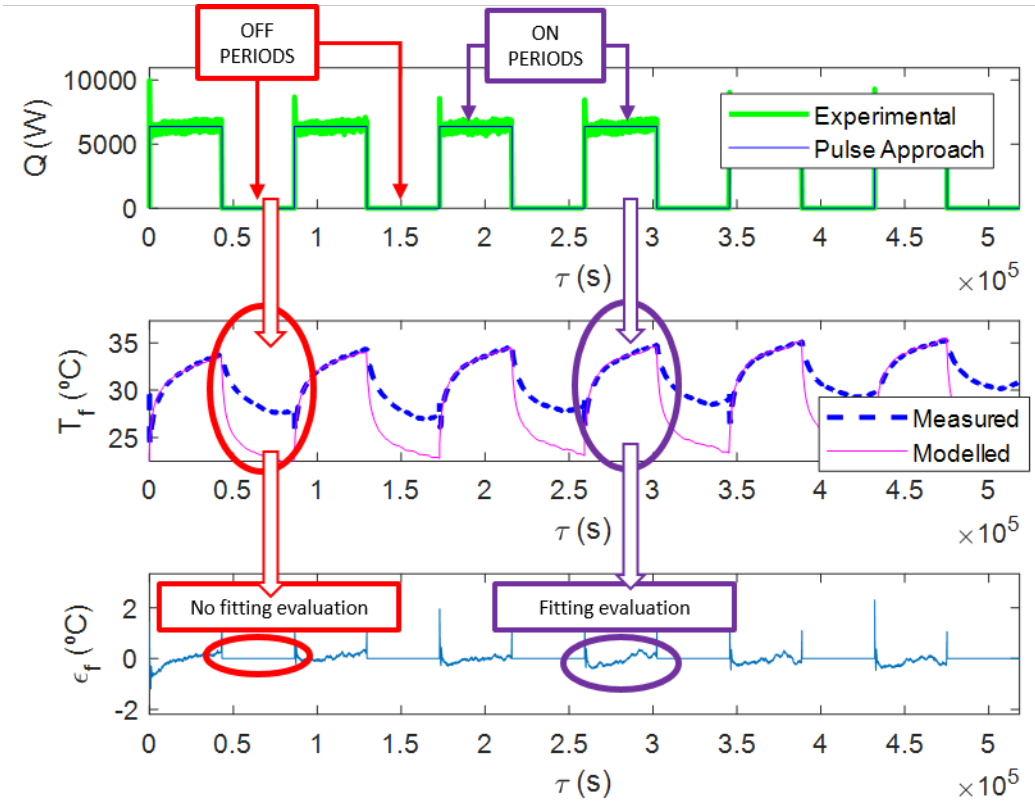

(7.a)

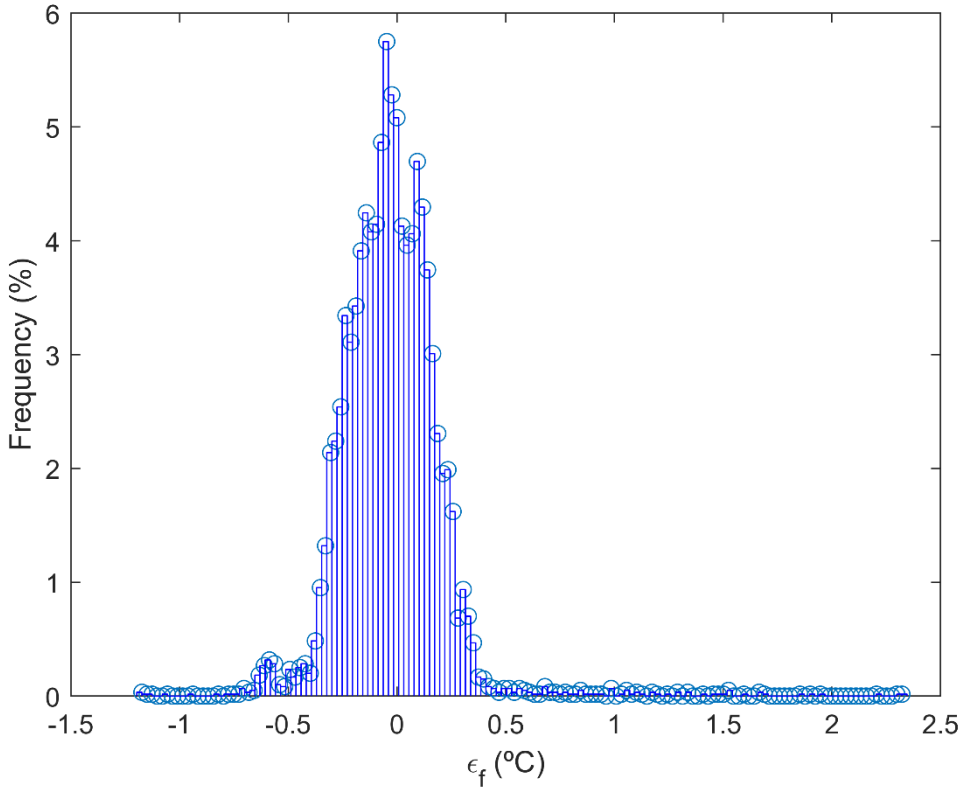

(7.b)

Figure 7. Results for test nr. 1: a) Complete period; b) Histogram of the deviation error ε_f

In Fig. 8, an additional intermittent proof is also presented (case 2), with very short time intervals of the heat pulses. These intervals are representative of that first loop period associated to the fluid circulation, where differences might be higher.

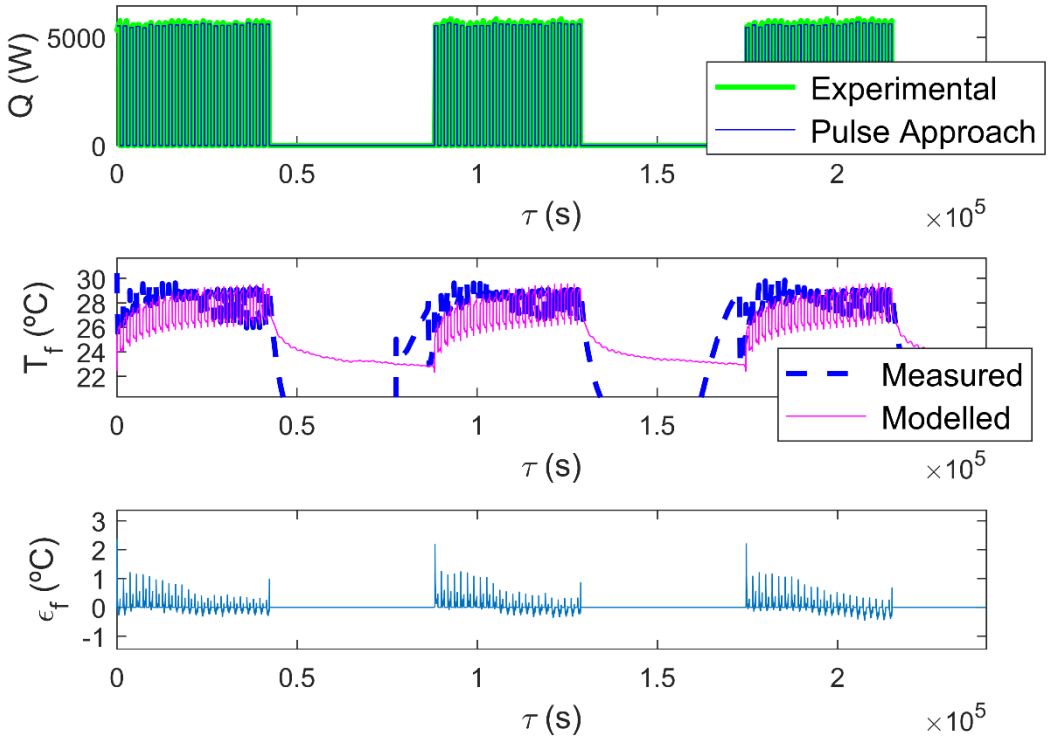

(8.a)

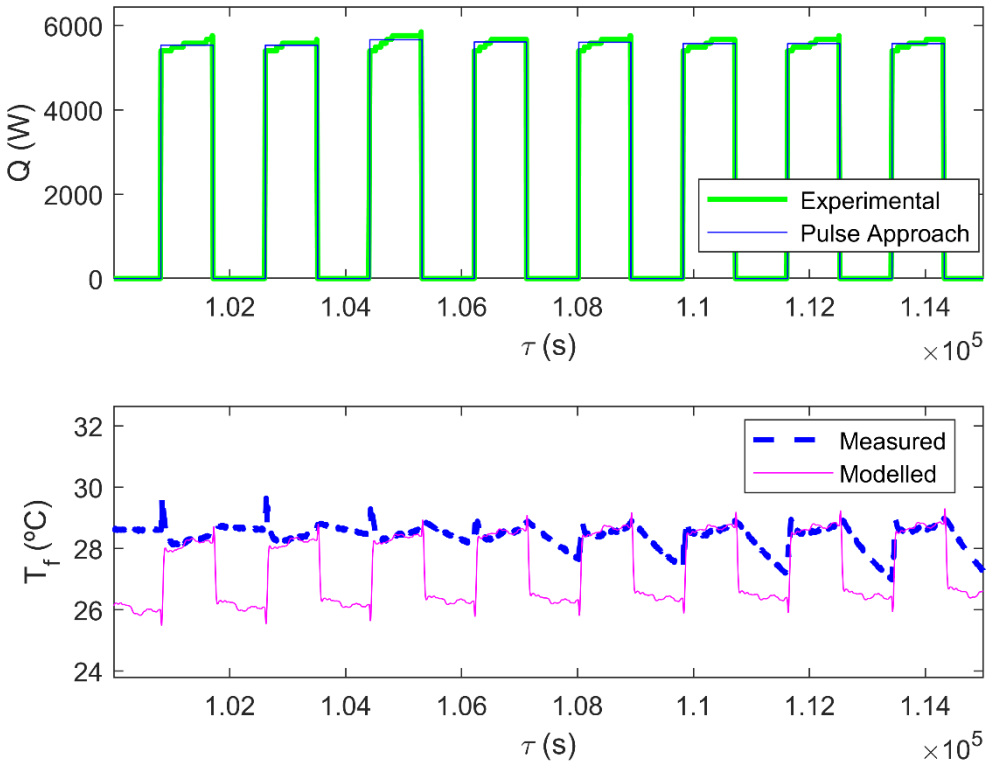

(8.b)

Figure 8. Results for test nr. 2: a) Complete period; b) Detail

In the following proof (case 3, see fig. 9), the ECU has been programmed to establish pulses of constant inlet temperature, in order to reproduce an arbitrary heat rate along time.

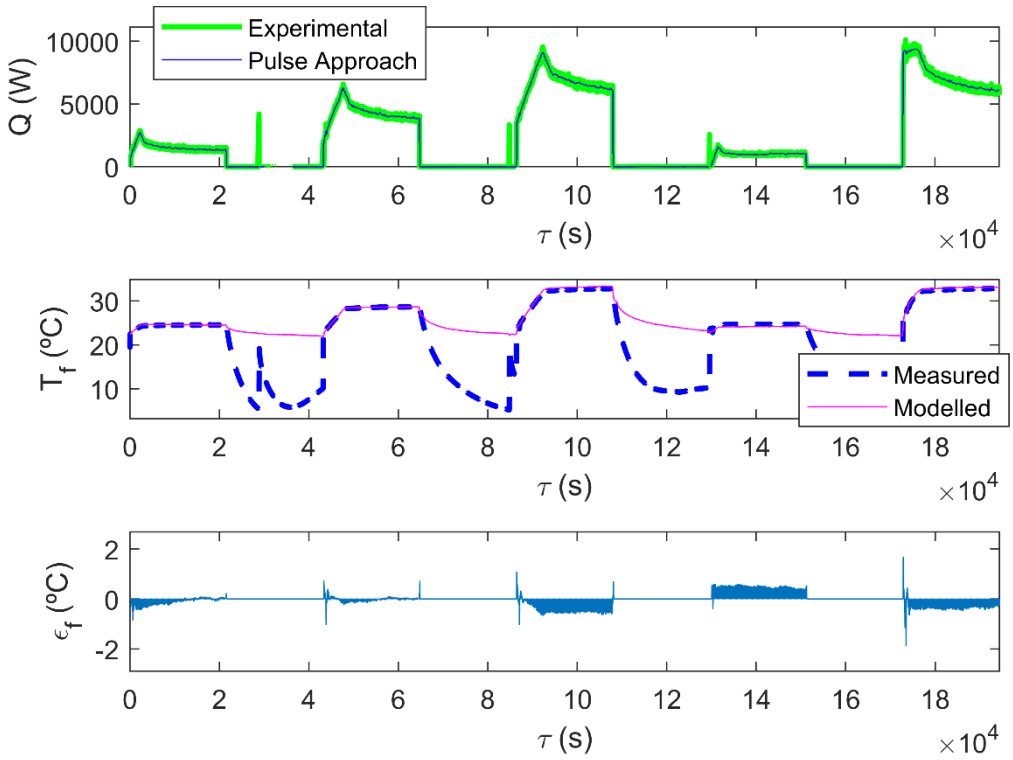

Figure 9. Results for test nr. 3

It can be observed the similar tendency that model provides for T_f, being quite well fitted, for those intervals "on" where the transfer fluid circulates. The complex load aggregation is solved satisfactorily by the model in all of the cases, observing excellent results. Average measured temperatures vary in "off" periods depending on the ambient conditions, which make them to rise or down, but do not represents the internal diffusion into tubes along depth, because of the fluid stop. At these "off" intervals, the model takes into account negative heat steps into the aggregate heat load, thus information from simulations seems to be more reliable that measurements in these periods. Once the fluid starts to flow newly in an "on" stage, the temperature trend is recovered quickly, being quite well adjusted after a small interval of time.

Up to this point, volumetric flow rate was the same as for the TRT. Following the Table 1, the rest of tests have been carried out with other value for it (20l/min). Results can be seen in Figs. 10 to 12. The two first tests correspond to intermittent behavior of heat pulses, while the last one takes a variable heat injection along time. The trends are also quite well adjusted.

In these last cases, a very little change appears in R_b with respect to that original R_{b0}, due to the film coefficient fluid-inner tube wall. Its effects are negligible, as can be seen. Moreover, the first loop step that appears in Fig. 6 (for about 900s) has a quite low influence in the final model results. Tendencies are maintained, thus the approach has not been apparently disturbed for this change in the volumetric flow rate.

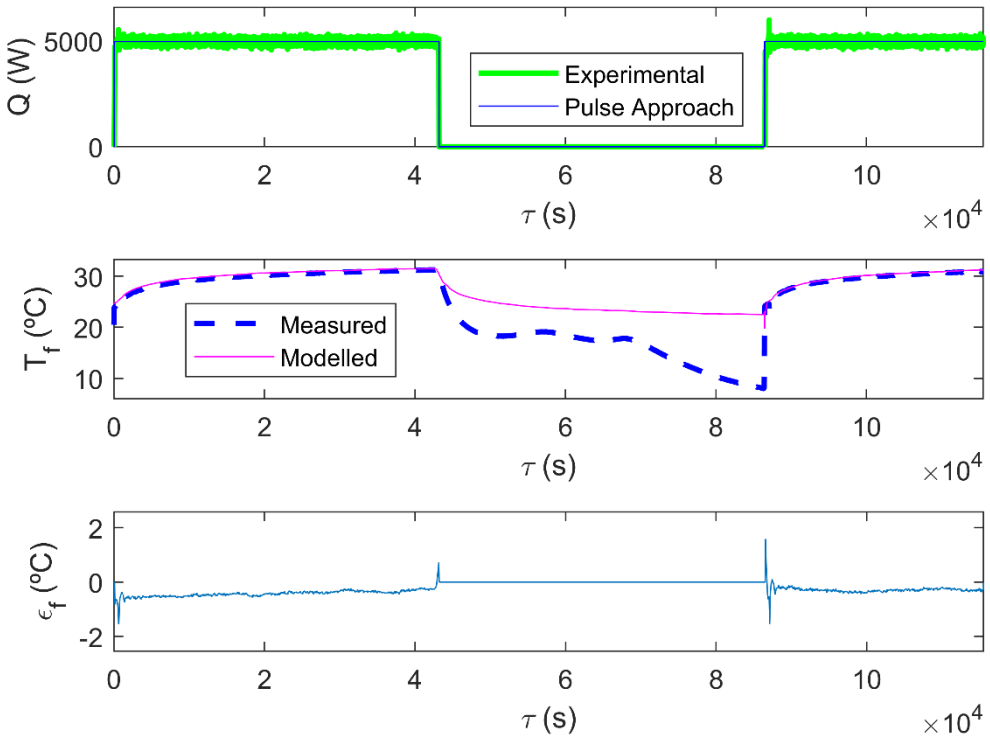

Figure 10. Results for test nr. 4

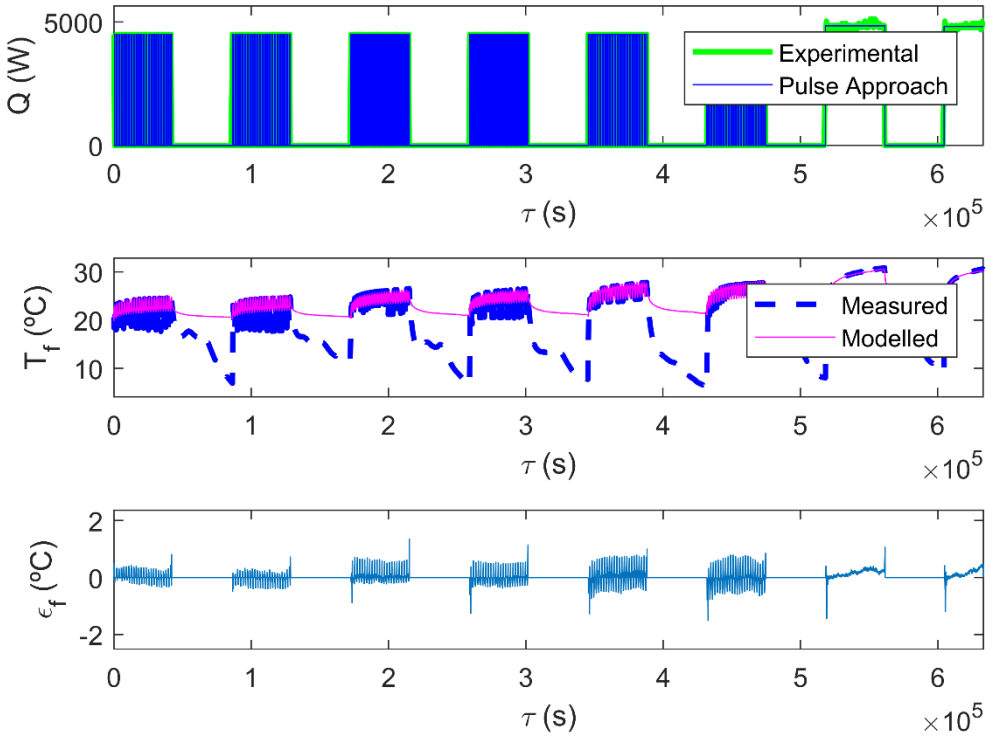

(11.a)

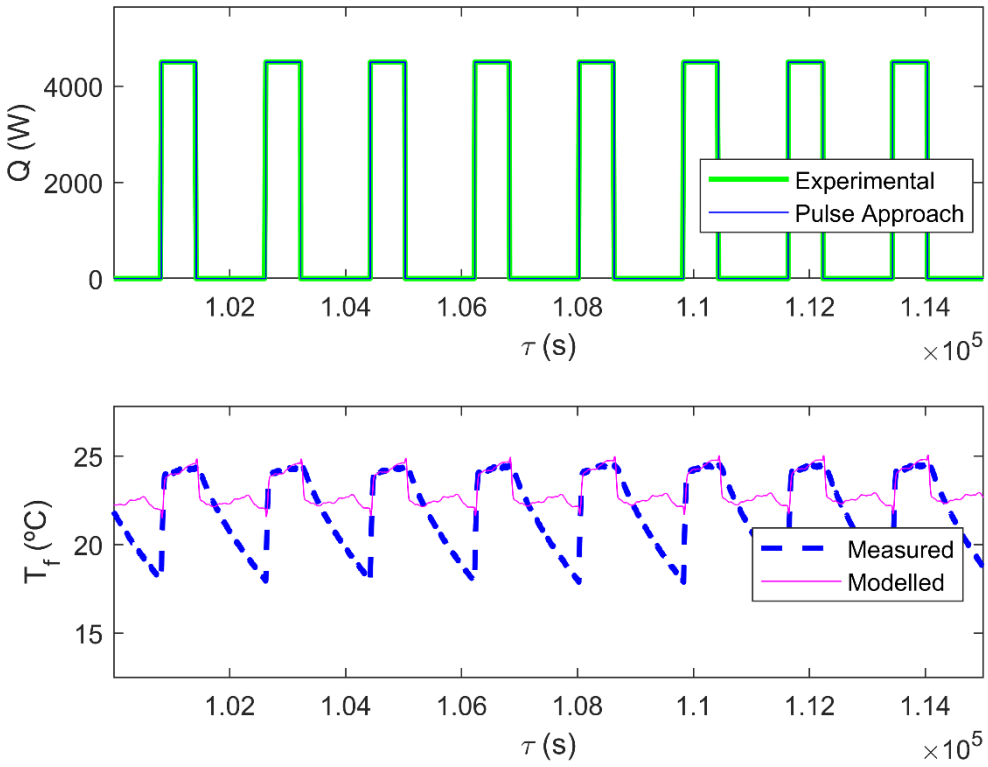

(11.b)

Figure 11. Results for test nr. 5: a) Complete period; b) Detail

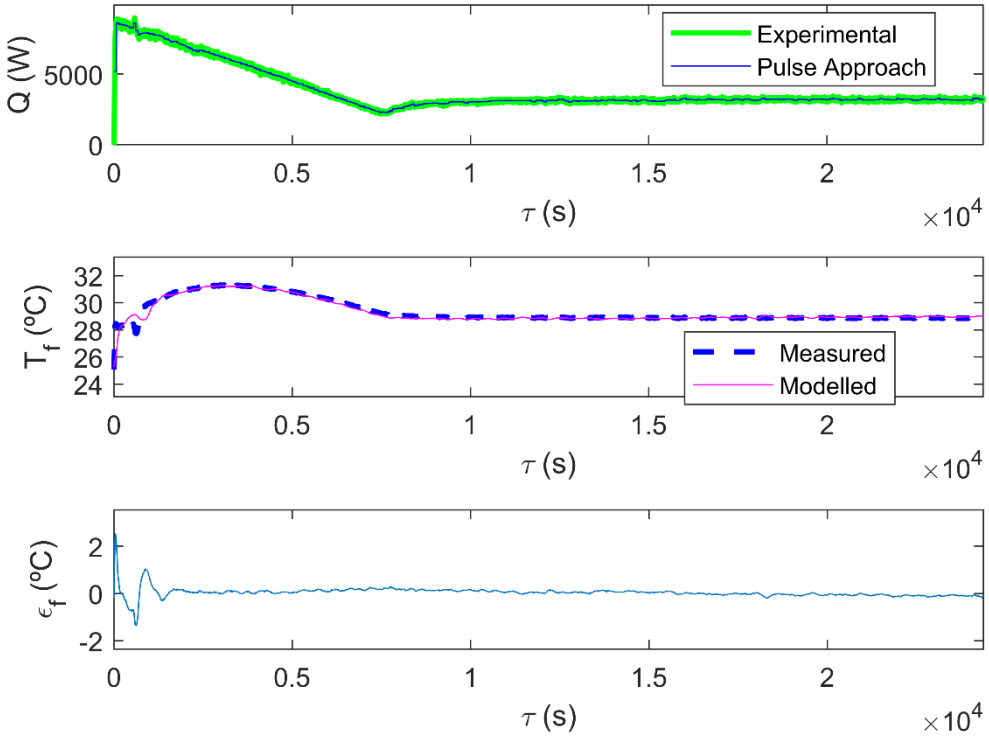

Figure 12. Results for test nr. 6

In order to show the accuracy of all these results, some stochastic terms of the estimation error of T_f are presented in Table 2, demonstrating the high reliability of the method.

Table 2. Average fluid temperature error estimations

Test Nr.	Mean (ºC)	Standard deviation (ºC)	Mode (ºC)	Median (ºC)	Coefficient of determination r^2 (dimensionless)
1	-0.03	0.23	-0.047	-0.036	0.98
2	0.007	0.21	-0.085	-0.03	0.94
3	-0.08	0.36	0.005	-0.11	0.99
4	-0.35	0.15	-0.28	-0.34	0.94
5	0.012	0.26	0.028	-0.004	0.96
6	0.04	0.21	0.061	0.04	0.94

Previous experiences validate their results based on: i) synthetic data, including several heat pulses along time; ii) experimental data, but for single heating pulses, without jumps in them. Thus, mean errors between 0,025ºC to 0,1ºC have been reported [14, 18, 19, 40]. In nearly all of the cases of this study, errors are included in that range, and even two of them present better results (cases nr. 2 and 5). For the worst of them (case nr. 4), it would be necessary a better adjusting of the heat rate step at the previous time before the test, which may reduce the mean value of that temperature error up to a 0,02ºC. In any case, it is important to remark that the tests carried out in this work correspond to quite extreme experiments with short heat pulses. Only a few of similar trials have been described, such as in [7].

The excellent approach presented in Figs (7) to (12) and Table 2 demonstrates the high reliability of using a local experiment-based STGF into a single borehole. Model adjustments to those additional experiments validate the proposed method. As it can be seen in the results, variations in both volumetric flow and unitary heat rates can be reproduced adequately. Thus, TRT measurements along the entire experiment can be used, while before, a large amount of the information was discarded. From now, a local experimentally STGF can be quickly supplied, and directly used to design or optimize a GSHP system, also avoiding high precomputing times. Effects that R_b causes are negligible for short times, although it is important to secure a reliable value, because its influence is significate in the long-term, as can be seen in eq. (9).

All the procedure has been repeated taking into account a p-linear average for determining T_f [29]. As a result of the TRT analysis, λ_s=1.84 W/mK (2% lower than before) and R_b = 0.131mK/W (7% lower than before) and another STGF profile has been performed. Results for the set of experiments are quite well fitted in general. Nevertheless, for those cases with very short cycles (cases 2 and 5), the adjustments decay, with r^2 around 0.9. It implies that the direct average approach from temperature measurements of the TRT is better to reflect the transient behavior of the first interval time of the test, which is reproduced later by means of the STGF. In any case, the p-linear average (p tending to -1) is recommended for a better determination of Rb using TRT data, although its repercussion is minimum in this study, so appreciable differences have not been observed.

Thus, for a vertical GHE design procedure, it must be realized of the designer's experience and the local market about drillings and materials, in order to a previous establishment of the dimensions of a single borehole, and its inner configuration: the STGF has a local effect, and will serve to evaluate the behavior of any borehole with the same characteristics to that tested: i) well diameter and material of filling (such as bentonite, preparing the mixing in the same way as the tested borehole); ii) tubes: material, diameter, thickness and type of tube (single U-tube, double U-tube, and so on); iii) transfer fluid: being water, mixes water-glycol with known proportions, and so on. Over this basic composition, boreholes depth, heat pulses and volumetric flows can be changed for an optimal design into a certain GHE configuration of several boreholes.

Some limitations do not allow generalizing this STGF, because it represents the local behavior of the soil and borehole where it is tested. Thus, it cannot be applied to: i) another different configuration than of that tested single borehole (e.g. another filling material); ii) other places with different thermal characteristics, even with the same borehole characteristics (material, geometries, and so on).

4.- Conclusions

The main conclusion that this study shows is the robustness of the proposed method, providing a reliable local STGF based on measurements from a TRT. It can also be concluded:

- The low deviation errors associated with the model validation from such extreme experiments ensure the reliability of the proposed method.
- The experimentally obtained temperature response factor characterizes the thermal behavior in a single well, although it can be easily extended to a complete field with any configuration.
- The STGF curve shows sufficient precision, as it contains intrinsic information about local terrain conditions and backfill materials. Even assuming certain errors in the initial thermal characterization, these are minimized when executing the model. The accurate results presented in this work (see figs. 7-12) show the goodness of its use.
- This strictly local application limits its use to the place where the TRT is performed, so the results cannot be generalized. It can only be applied to a set of perforations with the same characteristics as the ones tested: dimensions, materials in the well and transfer fluid. In any case, this should not be a problem, as a prior TRT is always recommended before designing a GHE.
- The high reliability of the function allows studies with intermittent operation, variable heat rates, fluid flow rates and operating intervals, allowing an optimal design of any GSHP.
- This function can be obtained easily and quickly, with a very low computational load. It represents an additional advantage over the previous methods.
- The method extends the application of data measured by a TRT, giving it a greater impact.
- The last moment of the TRT corresponds to the connection point between this experimentally based STGF and an analytical LTGF (widely validated), where both values match. It involves having a full temperature response factor function that includes short and long-term behavior, to be used at the design stage of any GHE configuration in a GSHP system

In a future study, it may be interesting to search a function to depicts a variable borehole resistance, which must reach, by an asymptotic way, the constant value of R_{b0} at the connecting

615 point between STGF and LTGF. It would complement an STGF with a different profile from that
616 presented here, with no negative values. Besides, as this process could be repeated at several
617 locations with different thermal properties, results can be useful to search for a procedure to
618 generalize this function. For this purpose, it is necessary to evaluate the relationships between
619 thermal properties and those profiles.

620 **Acknowledgments**

621 This work has been supported by a research contract at the University of Jaén (code 2439).

622 **References**

623 [1] Gamage K, Fahrioglu M The current technological status of ground source heat pump systems
624 and their potential use in Northern Cyprus. Int J Wind Renew Energy 2014;3:39-48.

625 [2] Demirbas A Global geothermal energy scenario by 2040. Energy Sources, Part A
626 2008;30:1890-5.

627 [3] Fridleifsson IB, Bertani R, Huenges E, Lund JW, Ragnarsson A, Rybach L The possible role
628 and contribution of geothermal energy to the mitigation of climate change. 2008;20:59-80.

629 [4] Kharseh M, Altorkmany L, Al-Khawaj M, Hassani F Warming impact on energy use of HVAC
630 system in buildings of different thermal qualities and in different climates. Energy conversion and
631 management 2014;81:106-11.

632 [5] Zhu N, Hu P, Xu L, Jiang Z, Lei F Recent research and applications of ground source heat
633 pump integrated with thermal energy storage systems: A review. Appl Therm Eng 2014;71:142-
634 51.

635 [6] Choi JC, Lee SR, Lee DS Numerical simulation of vertical ground heat exchangers: intermittent
636 operation in unsaturated soil conditions. Comput Geotech 2011;38:949-58.

637 [7] Miyara A Thermal performance investigation of several types of vertical ground heat
638 exchangers with different operation mode. Appl Therm Eng 2012;33:167-74.

639 [8] Cui P, Yang H, Fang Z Numerical analysis and experimental validation of heat transfer in
640 ground heat exchangers in alternative operation modes. Energy Build 2008;40:1060-6.

641 [9] Gao Q, Li M, Yu M Experiment and simulation of temperature characteristics of intermittently-
642 controlled ground heat exchanges. Renewable Energy 2010;35:1169-74.

643 [10] Yang H, Cui P, Fang Z Vertical-borehole ground-coupled heat pumps: A review of models
644 and systems. Appl Energy 2010;87:16-27.

645 [11] Eskilson P Thermal analysis of heat extraction boreholes [Ph.D. Thesis]. : Department of
646 Mathematical Physics, Lund Univ., 1987.

647 [12] Kummert M, Bernier M Sub-hourly simulation of residential ground coupled heat pump
648 systems. Building Services Engineering Research and Technology 2008;29:27-44.

649 [13] Partenay V, Riederer P, Salque T, Wurtz E The influence of the borehole short-time response
650 on ground source heat pump system efficiency. Energy Build 2011;43:1280-7.

651 [14] Javed S, Claesson J New analytical and numerical solutions for the short-term analysis of
652 vertical ground heat exchangers. ASHRAE Trans 2011;117:3-12.

653 [15] Pasquier P, Marcotte D Short-term simulation of ground heat exchanger with an improved
654 TRCM. Renewable Energy 2012;46:92-9.

655 [16] De Carli M, Tonon M, Zarrella A, Zecchin R A computational capacity resistance model
656 (CaRM) for vertical ground-coupled heat exchangers. Renewable Energy 2010;35:1537-50.

657 [17] Ruiz-Calvo F, De Rosa M, Acuña J, Corberán J, Montagud C Experimental validation of a
658 short-term Borehole-to-Ground (B2G) dynamic model. Appl Energy 2015;140:210-23.

659 [18] Brussieux Y, Bernier M Hybrid model for generating short-time g-functions. 2018:48-58.
660 doi:10.22488/okstate.18.000011.

661 [19] Pasquier P, Zarrella A, Labib R Application of artificial neural networks to near-instant
662 construction of short-term g-functions. Appl Therm Eng 2018;143:910-21.

663 [20] Yavuzturk C, Spitler JD A short time step response factor model for vertical ground loop heat
664 exchangers. ASHRAE Trans 1999;105:475-85.

665 [21] Liu X, Hellstrom G Enhancements of an integrated simulation tool for ground-source heat
666 pump system design and energy analysis. Proceedings of Ecostock 2006.

667 [22] Fisher DE, Rees SJ, Padhmanabhan S, Murugappan A Implementation and validation of
668 ground-source heat pump system models in an integrated building and system simulation
669 environment. HVAC&R Research 2006;12:693-710.

670 [23] Li M, Lai AC Parameter estimation of in-situ thermal response tests for borehole ground heat
671 exchangers. Int J Heat Mass Transfer 2012;55:2615-24.

672 [24] Witte HJ, Van Gelder GJ, Spitier JD In situ measurement of ground thermal conductivity: a
673 Dutch perspective. ASHRAE Trans 2002;108:263.

674 [25] Beier RA Vertical temperature profile in ground heat exchanger during in-situ test. Renewable
675 Energy 2011;36:1578-87.

676 [26] Gehlin S, Hellström G Comparison of four models for thermal response test evaluation.
677 ASHRAE Trans 2003;109:135-46.

678 [27] Sharqawy M, Mokheimer E, Habib M, Badr H, Said S, Al-Shayea N Energy, exergy and
679 uncertainty analyses of the thermal response test for a ground heat exchanger. Int J Energy Res
680 2009;33:582-92.

681 [28] Bozzoli F, Pagliarini G, Rainieri S, Schiavi L Estimation of soil and grout thermal properties
682 through a TSPEP (two-step parameter estimation procedure) applied to TRT (thermal response
683 test) data. Energy 2011;36:839-46.

684 [29] Marcotte D, Pasquier P On the estimation of thermal resistance in borehole thermal
685 conductivity test. Renewable Energy 2008;33:2407-15.

686 [30] Zhang X, Zhang T, Li B, Jiang Y Comparison of Four Methods for Borehole Heat Exchanger
687 Sizing Subject to Thermal Response Test Parameter Estimation. Energies 2019;12:4067.

688 [31] Casanova-Peláez P, Palomar-Carnicero JM, López-García R, Cruz-Peragón F Desarrollo de
689 equipo para la realización de test de respuesta térmica del terreno (TRT) en instalaciones
690 geotérmicas. Dyna 2014;89:316-24.

691 [32] Gehlin S, Nordell B Determining undisturbed ground temperature for thermal response test.
692 2003;109:151-6.

693 [33] Sanner B, Hellström G, Spitler J, Gehlin S Thermal response test–current status and world-
694 wide application. 2005;200.

695 [34] Hellström G Ground heat storage: thermal analyses of duct storage systems [Ph.D. Thesis].
696 : Department of Mathematical Physics, Lund Univ., 1991.

697 [35] Abramovich M, Stegun I Handbook of Mathematical Functions with Formulas, graphs and
698 mathematical Tables, National Bureau of Standarts. Appl.Math.series 1964;55.

699 [36] Diao N, Zeng H, Fang Z Improvement in modeling of heat transfer in vertical ground heat
700 exchangers. HVAC&R Research 2004;10:459-70.

701 [37] Yavuzturk C, Spitler JD, Rees SJ A transient two-dimensional finite volume model for the
702 simulation of vertical U-tube ground heat exchangers. ASHRAE Trans 1999;105:465.

[38] Marcotte D, Pasquier P, Sheriff F, Bernier M The importance of axial effects for borehole design of geothermal heat-pump systems. Renewable Energy 2010;35:763-70.

[39] Lamarche L, Kajl S, Beauchamp B A review of methods to evaluate borehole thermal resistances in geothermal heat-pump systems. Geothermics 2010;39:187-200.

[40] Xu X, Spitler JD Modeling of vertical ground loop heat exchangers with variable convective resistance and thermal mass of the fluid. Proceedings of Ecostock 2006.

[41] Pahud D Geothermal energy and heat storage. 2002:1-133.

Table captions

Figure captions